Photonic chip based transmitter optimization and receiver demultiplexing of a 1.28 Tbit/s OTDM signal

Vo, T.D.; Hu, Hao; Galili, Michael; Palushani, Evarist; Xu, Jing; Oxenløwe, Leif Katsuo; Madden, S.J.; Choi, D.Y.; Bulla, D.A.P.; Pelusi, M.D.; Schröder, J.; Luther-Davies, B.; Eggleton, B.J.

Published in:
Optics Express

Link to article, DOI:
10.1364/OE.18.017252

Publication date:
2010

Document Version
Publisher's PDF, also known as Version of record

Photonic chip based transmitter optimization and receiver demultiplexing of a 1.28 Tbit/s OTDM signal

T. D. Vo,[1,*] H. Hu,[2] M. Galili,[2] E. Palushani,[2] J. Xu,[2] L. K. Oxenløwe,[2] S. J. Madden,[3] D.-Y. Choi,[3] D. A. P. Bulla,[3] M. D. Pelusi,[1] J. Schröder,[1] B. Luther-Davies[3], and B. J. Eggleton[1]

[1]*ARC Centre for Ultrahigh bandwidth Devices for Optical Systems (CUDOS), Institute of Photonics and Optical Science (IPOS), School of Physics, University of Sydney, New South Wales 2006, Australia*
[2]*DTU Fotonik, Technical University of Denmark, DK-2800 Kgs. Lyngby, Denmark*
[3]*ARC Centre for Ultrahigh bandwidth Devices for Optical Systems (CUDOS), Laser Physics Centre, Australian National University, Canberra ACT 0200, Australia*
**trungvo@physics.usyd.edu.au*

Abstract: We demonstrate chip-based Tbaud optical signal processing for all-optical performance monitoring, switching and demultiplexing based on the instantaneous Kerr nonlinearity in a dispersion-engineered As_2S_3 planar waveguide. At the Tbaud transmitter, we use a THz bandwidth radio-frequency spectrum analyzer to perform all-optical performance monitoring and to optimize the optical time division multiplexing stages as well as mitigate impairments, for example, dispersion. At the Tbaud receiver, we demonstrate error-free demultiplexing of a 1.28 Tbit/s single wavelength, return-to-zero signal to 10 Gbit/s via four-wave mixing with negligible system penalty (< 0.5 dB). Excellent performance, including high four-wave mixing conversion efficiency and no indication of an error-floor, was achieved. Our results establish the feasibility of Tbaud signal processing using compact nonlinear planar waveguides for Tbit/s Ethernet applications.

OCIS codes: (070.4340) Nonlinear optical signal processing; (190.4360) Nonlinear optics, devices; (320.7110) Ultrafast nonlinear optics.

References and links

1. H. C. Hansen Mulvad, L. K. Oxenløwe, M. Galili, A. T. Clausen, L. Grüner-Nielsen, and P. Jeppesen, "1.28 Tbit/s single-polarisation serial OOK optical data generation and demultiplexing," Electron. Lett. **45**(5), 280–281 (2009).
2. H. Ji, H. Hu, M. Galili, L. K. Oxenløwe, M. Pu, K. Yvind, J. M. Hvam, and P. Jeppesen, "Optical Waveform Sampling and Error-free Demultiplexing of 1.28 Tbit/s Serial Data in a Silicon Nanowire," in Proc. Optical Fiber Communication Conference (OFC), San Diego, USA, 2010 (Postdeadline Paper).
3. H. C. H. Mulvad, M. Galili, L. K. Oxenløwe, H. Hu, A. T. Clausen, J. B. Jensen, C. Peucheret, and P. Jeppesen, "Demonstration of 5.1 Tbit/s data capacity on a single-wavelength channel," Opt. Express **18**(2), 1438–1443 (2010).
4. A. D. Ellis, J. Zhao, and D. Cotter, "Approaching the Non-Linear Shannon Limit," J. Lightwave Technol. **28**(4), 423–433 (2010).
5. M. Nakazawa, T. Yamamoto, and K. R. Tamura, "1.28 Tbit/s-70 km OTDM transmission using third- and fourth-order simultaneous dispersion compensation with a phase modulator," Electron. Lett. **36**(24), 2027–2029 (2000).
6. M. Nakazawa, E. Yoshida, T. Yamamoto, E. Yamada, and A. Sahara, "TDM single channel 640Gbit/s transmission experiment over 60 km using 400fs pulse train and walk-off free, dispersion flattened nonlinear optical loop mirror," Electron. Lett. **34**(9), 907–908 (1998).
7. H. G. Weber, S. Ferber, M. Kroh, C. Schmidt-Langhorst, R. Ludwig, V. Marembert, C. Boerner, F. Futami, S. Watanabe, and C. Schubert, "Single channel 1.28 Tbit/s and 2.56 Tbit/s DQPSK transmission," Electron. Lett. **42**(3), 178–179 (2006).
8. C. Schmidt-Langhorst, R. Ludwig, D.-D. Groß, L. Molle, M. Seimetz, R. Freund, and C. Schubert, "Generation and Coherent Time-Division Demultiplexing of up to 5.1 Tb/s Single-Channel 8-PSK and 16-QAM Signals," in Proc. Optical Fiber Communication Conference (OFC), San Diego, USA, 2009 (Postdeadline Paper).

#126238 - $15.00 USD Received 30 Mar 2010; revised 11 Jul 2010; accepted 16 Jul 2010; published 29 Jul 2010

9. T. Inoue, and S. Namiki, "Pulse compression techniques using highly nonlinear fibers," Laser Photon. Rev. **2**(1–2), 83–99 (2008).
10. J. Hansryd, P. A. Andrekson, M. Westlund, J. Li, and P.-O. Hedekvist, "Fiber-Based Optical Parametric Amplifiers and Their Applications," IEEE J. Sel. Top. Quantum Electron. **8**(3), 506–520 (2002).
11. J. Li, A. Berntson, and G. Jacobsen, "Polarization-Independent Optical Demultiplexing Using XPM-Induced Wavelength Shifting in Highly Nonlinear Fiber," IEEE Photon. Technol. Lett. **20**(9), 691–693 (2008).
12. M. Matsumoto, "A Fiber-Based All-Optical 3R Regenerator for DPSK Signals," IEEE Photon. Technol. Lett. **19**(5), 273–275 (2007).
13. G. T. Zhou, K. Xu, J. Wu, C. Yan, Y. Su, and J. T. Lin, "Self-Pumping Wavelength Conversion for DPSK Signals and DQPSK Generation Through Four-Wave Mixing in Highly Nonlinear Optical Fiber," IEEE Photon. Technol. Lett. **18**(22), 2389–2391 (2006).
14. M. D. Pelusi, F. Luan, E. Magi, M. R. Lamont, D. J. Moss, B. J. Eggleton, J. S. Sanghera, L. B. Shaw, and I. D. Aggarwal, "High bit rate all-optical signal processing in a fiber photonic wire," Opt. Express **16**(15), 11506–11512 (2008).
15. L. B. Fu, M. Rochette, V. G. Ta'eed, D. J. Moss, and B. J. Eggleton, "Investigation of self-phase modulation based optical regeneration in single mode As_2Se_3 chalcogenide glass fiber," Opt. Express **13**(19), 7637–7644 (2005).
16. R. J. Manning, A. D. Ellis, A. J. Poustie, and K. J. Blow, "Semiconductor laser amplifiers for ultrafast all-optical signal processing," J. Opt. Soc. Am. B **14**(11), 3204–3216 (1997).
17. E. Tangdiongga, Y. Liu, H. de Waardt, G. D. Khoe, A. M. J. Koonen, H. J. S. Dorren, X. Shu, and I. Bennion, "All-optical demultiplexing of 640 to 40 Gbits/s using filtered chirp of a semiconductor optical amplifier," Opt. Lett. **32**(7), 835–837 (2007).
18. L. K. Oxenlwe, F. Gomez, C. Ware, S. Kurimura, H. C. H. Mulvad, M. Galili, H. Nakajima, J. Ichikawa, D. Erasme, A. T. Clausen, and P. Jeppesen, "640-Gbit/s Data Transmission and Clock Recovery Using an Ultrafast Periodically Poled Lithium Niobate Device," J. Lightwave Technol. **27**(3), 205–213 (2009).
19. M. D. Pelusi, T. D. Vo, F. Luan, S. J. Madden, D.-Y. Choi, D. A. P. Bulla, B. Luther-Davies, and B. J. Eggleton, "Terahertz bandwidth RF spectrum analysis of femtosecond pulses using a chalcogenide chip," Opt. Express **17**(11), 9314–9322 (2009).
20. M. Pelusi, F. Luan, T. D. Vo, M. R. E. Lamont, S. J. Madden, D. A. Bulla, D. Y. Choi, B. Luther-Davies, and B. J. Eggleton, "Photonic-chip-based radio-frequency spectrum analyser with terahertz bandwidth," Nat. Photonics **3**(3), 139–143 (2009).
21. M. D. Pelusi, V. G. Ta'eed, M. R. E. Lamont, S. Madden, D.-Y. Choi, B. Luther-Davies, and B. J. Eggleton, "Ultra-High Nonlinear As_2S_3 Planar Waveguide for 160-Gb/s Optical Time-Division Demultiplexing by Four-Wave Mixing," IEEE Photon. Technol. Lett. **19**(19), 1496–1498 (2007).
22. M. Galili, J. Xu, H. C. Mulvad, L. K. Oxenløwe, A. T. Clausen, P. Jeppesen, B. Luther-Davies, S. Madden, A. Rode, D.-Y. Choi, M. Pelusi, F. Luan, and B. J. Eggleton, "Breakthrough switching speed with an all-optical chalcogenide glass chip: 640 Gbit/s demultiplexing," Opt. Express **17**(4), 2182–2187 (2009).
23. T. D. Vo, H. Hu, M. Galili, E. Palushani, J. Xu, L. K. Oxenløwe, S. J. Madden, D. Y. Choi, D. A. P. Bulla, M. D. Pelusi, J. Schröder, B. Luther-Davies, and B. J. Eggleton, "Photonic Chip Based 1.28 Tbaud Transmitter Optimization and Receiver OTDM Demultiplexing," in Proc. Optical Fiber Communication Conference (OFC), San Diego, USA, 2010 (Postdeadline Paper).
24. T. D. Vo, M. D. Pelusi, J. Schröder, F. Luan, S. J. Madden, D.-Y. Choi, D. A. P. Bulla, B. Luther-Davies, and B. J. Eggleton, "Simultaneous multi-impairment monitoring of 640 Gb/s signals using photonic chip based RF spectrum analyzer," Opt. Express **18**(4), 3938–3945 (2010).
25. T. D. Vo, M. D. Pelusi, J. Schröder, B. Corcoran, and B. J. Eggleton, "Multi-Impairment Monitoring at 320 Gb/s based on Cross Phase Modulation Radio-Frequency Spectrum Analyzer," IEEE Photon. Technol. Lett., (2010).
26. G. P. Agrawal, *Nonlinear Fiber Optics,* 3rd ed. (California: Academic Press, 2001).
27. C. Dorrer, and D. N. Maywar, "RF Spectrum Analysis of Optical Signals Using Nonlinear Optics," J. Lightwave Technol. **22**(1), 266–274 (2004).
28. S. J. Madden, D.-Y. Choi, D. A. Bulla, A. V. Rode, B. Luther-Davies, V. G. Ta'eed, M. D. Pelusi, and B. J. Eggleton, "Long, low loss etched $As_{(2)}S_{(3)}$ chalcogenide waveguides for all-optical signal regeneration," Opt. Express **15**(22), 14414–14421 (2007).
29. D.-Y. Choi, S. Madden, D. A. Bulla, R. Wang, A. Rode, and B. Luther-Davies, "Sub-micrometer thick, low-loss As_2S_3 planar waveguides for nonlinear optical devices," IEEE Photon. Technol. Lett. **22**(7), 495–497 (2010).
30. S. Song, C. T. Allen, K. R. Demarest, and R. Hui, "Intensity-Dependent Phase-Matching Effects on Four-Wave Mixing in Optical Fibers," J. Lightwave Technol. **17**(11), 2285–2290 (1999).
31. A. Prasad, C.-J. Zha, R.-P. Wang, A. Smith, S. Madden, and B. Luther-Davies, "Properties of $Ge_xAs_ySe_{1-x-y}$ glasses for all-optical signal processing," Opt. Express **16**(4), 2804–2815 (2008).
32. Y. Shani, C. H. Henry, R. C. Kistler, K. J. Orlowsky, and D. A. Ackerman, "Efficient coupling of a semiconductor laser to an optical fiber by means of a tapered waveguide on silicon," Appl. Phys. Lett. **55**(23), 2389–2391 (1989).
33. T. Shoji, T. Tsuchizawa, T. Watanabe, K. Yamada, and H. Morita, "Low loss mode size converter from 0.3 um square Si wire waveguides to singlemode fibres," Electron. Lett. **38**(25), 1669–1670 (2002).
34. S. H. Tao, J. Song, Q. Fang, M. B. Yu, G. Q. Lo, and D. L. Kwong, "Improving coupling efficiency of fiber-waveguide coupling with a double-tip coupler," Opt. Express **16**(25), 20803–20808 (2008).

#126238 - $15.00 USD Received 30 Mar 2010; revised 11 Jul 2010; accepted 16 Jul 2010; published 29 Jul 2010

1. Introduction

The growing demand for higher bandwidths is a major motivation behind the push to increase the per-channel transmission rate of optical systems. Recently, attention has focused on establishing the feasibility of Tbaud transmission for Tbit/s network applications [1, 2]. Optical time division multiplexing (OTDM) allows Tbaud symbol rates which can be combined with advanced modulation formats to achieve unprecedented capacity per-channel with efficient bandwidth utilization [3]. Successful Tbaud transmission requires three crucial building blocks: high-quality signal generation via OTDM; effective impairment monitoring and mitigation within the network; and efficient demultiplexing at the receiver end. In low symbol rate systems these functions are provided in the electrical domain by digital signal processing chip-sets. However, at Tbaud symbol rates all-optical approaches are the only solution due to the limitations imposed by the electronic bandwidth.

Single-channel Tbit/s transmission rates can be achieved by either increasing the symbol rate (baud-rate) of the channel or by using advanced (coherent) modulation formats, such as differential quadrature phase shift keying (DQPSK); m-aray phase shift keying (m-PSK); or m-aray quadrature amplitude shift keying (m-QAM) [4]. For maximum spectral efficiency and, thus, the highest data rate, it is best to combine the maximum possible symbol (baud) rate with the most efficient advanced modulation format. The first demonstration of a single-channel 1.28 Tbit/s transmission was in 2000 [5]. To achieve this bit rate Nakazawa and colleagues used polarization multiplexing of 640 Gbit/s on-off keying (OOK) transmission [6]. More recently, Weber *et al.* demonstrated 2.56 Tbit/s by taking advantage of the 2 bits per symbol of the DQPSK modulation format also in combination with polarization multiplexing [7]. Note that these experiments were based on 640 Gbaud symbol rate. The current record single-channel transmission rate is 5.1 Tbit/s and was achieved by both Schmidt-Langhorst *et al.* [8] and Mulvad *et al.* [3]. While Schmidt-Langhorst *et al.* exploited a multilevel modulation format (16-QAM, 4 bits per symbol) [8] and polarization multiplexing with 640 Gbaud symbol rate to achieve this high data-rate, Mulvad *et al.* demonstrated a breakthrough 1.28 Tbaud symbol rate which was encoded using the DQPSK modulation format and polarization multiplexed to reach 5.1 Tbit/s [3].

Apart from the difficulties in producing a Tbit/s signal, this high bit-rate poses significant challenges for signal processing and optical performance monitoring. Due to the bandwidth limitation (< 100 GHz) of conventional electronic switches, novel, all-optical techniques that overcome this limitation have been widely researched. Although highly nonlinear fiber [9–13] or fiber photonic wires [14, 15] have had considerable success as a platform for all-optical processing, a compact and monolithic, integrated solution that can incorporate multiple functionalities is advantageous. In particular, solutions based on highly nonlinear structures promise to deliver all-optical signal processing in compact integrated circuits. Amongst these semiconductor optical amplifiers [16, 17] offer enormous nonlinearities but suffer from free-carrier dynamics at high bit-rates which translates into a significant system penalty. Periodically poled $LiNbO_3$ [18] has been exploited in numerous high-bit rates experiments but requires temperature control and quasi-phase matching which is not always compatible with ultrafast processing. Chalcogenide (ChG) planar waveguides, on the other hand, do not suffer free-carrier absorption, are stable at room temperature and have a broad operating bandwidth [19] due to dispersion engineering. They are an ideal platform for Tbit/s bit-rate systems, because of their high nonlinear response γ, enabling very compact devices [20–22].

In this paper, we propose a scheme that uses photonic chips to perform all-optical signal processing at the nodes of a Tbit/s network [23]. We implemented this scheme demonstrating all-optical signal monitoring and optimization at the transmitter and ultra-fast switching at the receiver using a highly nonlinear dispersion-engineered planar ChG waveguide. The 1.28 Tbaud transmitter was implemented using OTDM and we performed optical performance monitoring (OPM) [24, 25] to measure and (via feedback) optimize dispersion and mitigate

#126238 - $15.00 USD Received 30 Mar 2010; revised 11 Jul 2010; accepted 16 Jul 2010; published 29 Jul 2010

impairments introduced by the misalignment of the OTDM multiplexing (MUX) stages. The photonic chip OPM offers many advantages, including high sensitivity, multi-impairment monitoring, and > 2.5 THz operating bandwidth [19, 20]. At the Tbaud receiver, we demonstrated error-free demultiplexing of a 1.28 Tbit/s single wavelength, OOK signal to 10 Gbit/s via four-wave mixing (FWM) with a low system penalty of < 0.5 dB. Excellent performance, including high FWM conversion efficiency and no indication of an error-floor, was achieved. This shows the great potential of these compact nonlinear ChG waveguides for Tbaud signal processing.

2. Tbaud optical system and planar waveguide characteristics

The working principle of the Tbaud transmitter and receiver system is shown in Fig. 1. At the transmitter a pulse train with sufficiently short pulses is encoded with data using a Mach-Zehnder (MZ) modulator before being multiplexed up to 1.28 Tbit/s in a seven-stage MUX. This high bit-rate OTDM signal is very sensitive to impairments such as dispersion, jitter and noise as well as environmental factors, e.g. temperature, which would lead to a misalignment of the MUX and may degrade the signal quality. The OPM was therefore used to continuously monitor the quality of the output signal from the transmitter. We fed the OPM features back to the MUX stages to optimize the signal and continuously mitigate signal impairments introduced by drift in the MUX. At the OTDM receiver, the high bit-rate signal was demultiplexed to the base rate and detected by a photodiode.

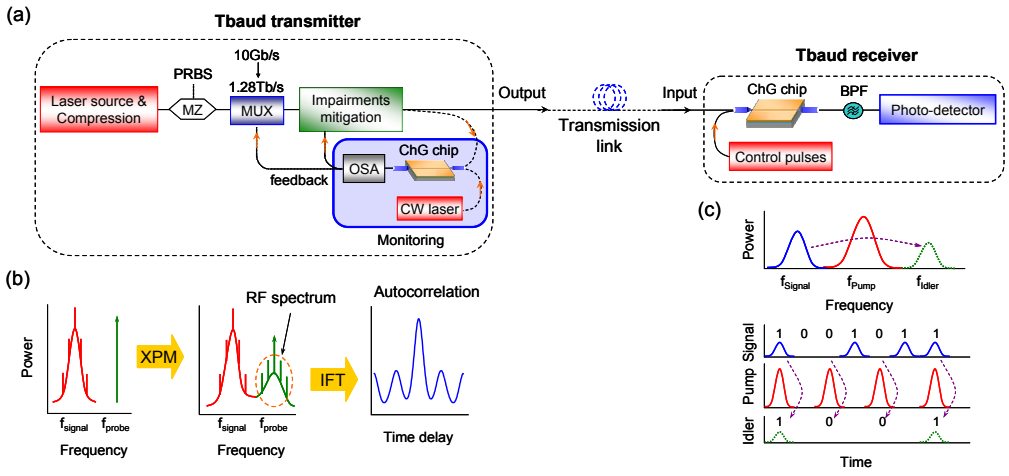

Fig. 1. (a) Diagram of Tbaud transmitter optimization and Tbaud receiver OTDM demultipexing. Schematics of (b) cross-phase modulation based RF spectrum analyzer for OPM and MUX optimization at the transmitter and (c) all-optical Tbaud demultiplexing.

The working principle of the OPM is shown in Fig. 1(b). When a signal under test (SUT) is co-propagated with a continuous wave (cw) probe laser, new frequencies will be generated around the probe due to cross phase modulation (XPM) [26] in the ChG waveguide. It can be shown that the optical spectrum of the probe modulated by XPM is equivalent to the power spectrum, or radio-frequency (RF) spectrum of the SUT [20, 27]. Based on the Weiner-Khintchine theorem, the autocorrelation (AC) waveform of the SUT is obtained by performing a numerical inverse Fourier transform (IFT) of the captured RF spectrum [19]. By exploiting the distinguishing features of the RF spectra and AC traces, impairments may effectively be monitored.

At the receiver end, the high bit-rate signal was demultiplexed to the base rate for detection with conventional electronics. The principle of this all-optical demultiplexer is shown in Fig. 1(c). The high bit-rate signal was co-propagated with pump control pulses operating at the base rate. By changing the delay between pump and signal we adjusted the

#126238 - $15.00 USD Received 30 Mar 2010; revised 11 Jul 2010; accepted 16 Jul 2010; published 29 Jul 2010

pump pulses to coincide with any desired channel of the high bit-rate signal. Due to FWM inside the ChG waveguide the chosen signal channel was converted to a new idler wavelength [26] and then extracted from the output via spectral filtering.

The key device in these monitoring and demultiplexing experiments is a 7 cm long dispersion engineered As_2S_3 planar waveguide whose micrograph image and characteristics are shown in Fig. 2. Details of the fabrication of this As_2S_3 planar waveguide have been described in [28, 29]. In order to offset the large material dispersion of about – 370 ps/nm/km, the As_2S_3 film thickness was reduced to ~0.85 μm resulting in a combined waveguide and material dispersion of ~29 ps/nm/km for the transverse-magnetic (TM) mode at 1550 nm [Fig. 2(c)]. The nonlinear coefficient γ of this waveguide at a wavelength of 1550 nm was therefore enhanced up to ~9900 /W/km. The optical micrograph and the numerical intensity mode profile of the TM mode are shown in Fig. 2(a) and 2(b). This short and low dispersion waveguide offers very low walk-off, thus enabling high measurement accuracy and excellent FWM conversion efficiency.

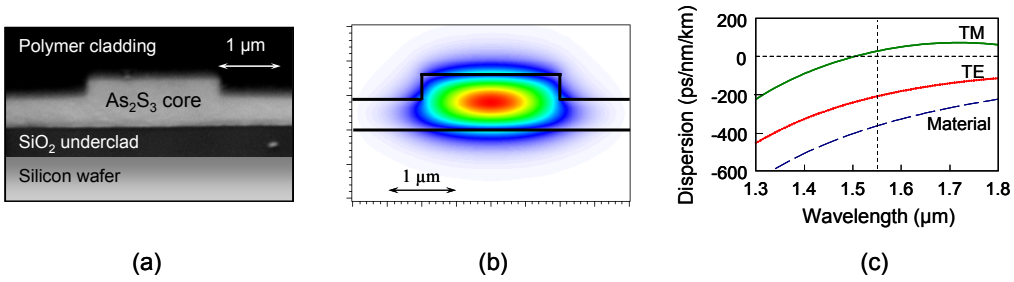

Fig. 2. (a) Optical micrograph image of an As_2S_3 planar waveguide cleaved facet. Numerical results showing (b) fundamental TM mode intensity profile and (c) group velocity dispersion of TM, TE mode and material dispersion for a 2 μm width planar waveguide.

3. Experimental setup

The experimental setup is shown in Fig. 3. Both 1.28 Tbit/s and 10 GHz pump pulses were generated from a 10 GHz erbium glass oscillator (ERGO) laser followed by a two-stage nonlinear pulse compression. In the first stage, the output from the ERGO laser was spectrally broadened by self-phase modulation (SPM) in a dispersion-flattened highly nonlinear fiber (HNLF) (length L = 400 m, dispersion D = –0.45 ps/nm/km, slope S = 0.006 ps/nm^2/km, and γ = 10.5 /W/km at 1550 nm). The signal and pump pulses were then generated by spectral filters at 1550 nm and 1573 nm respectively and compressed inside two different lengths of SMF fiber. This compression process was repeated in the second stage with 100 m (signal) and 200 m (pump) HNLF (D = –1.07 ps/nm/km, S = 0.004 ps/nm^2/km, and γ = 10.5 /W/km). The compressed 10 GHz pulse train centered at 1550 nm was then encoded with data using a MZ modulator and interleaved by a seven-stage multiplexing setup with 2^7 - 1 bit delay length to produce the 1.28 Tbit/s signal.

The 1.28 Tbit/s signal was tapped to allow its RF spectrum to be monitored using the XPM-based RF spectrum analyzer whose setup is shown in Fig. 3(b). The monitoring features were fed back to the MUX stages for signal optimization and impairment mitigation. Finally, Fig. 3(c) shows the experimental setup for demultiplexing the high bit-rate signal to the base rate for detection at the receiver end. The 1.28 Tbit/s signal (P_{ave} ~100 mW) and 10 GHz control pulses (P_{ave} ~60 mW) were coupled to the TM mode of a waveguide via lensed fibers with a 2.5 μm mode field diameter to take advantage of broadband operation of this mode. The total insertion loss of the chip was ~13 dB, comprising of ~5 dB free-space coupling loss per facet. Thus the total average power within the waveguide was estimated to be ~50 mW.

#126238 - $15.00 USD Received 30 Mar 2010; revised 11 Jul 2010; accepted 16 Jul 2010; published 29 Jul 2010

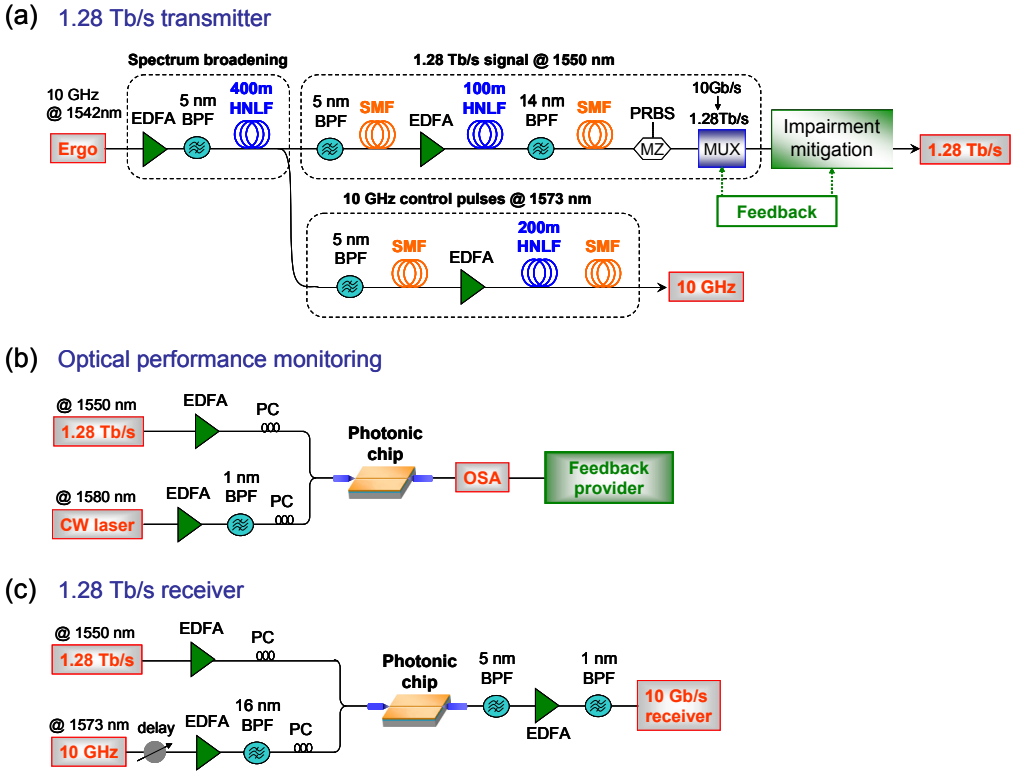

Fig. 3. (a) Experimental setup for 1. 28 Tbit/s transmitter. (b) optial performance monitoring for a 1.28 Tbit/s OOK signal for transmitter optimization and (c) 1.28 Tbit/s all-optical demultiplexing by FWM in a ChG planar waveguide.

4. Experimental results

At the transmitter, OPM features captured from the XPM based RF spectrum analyzer were exploited for Tbit/s signal optimization and maintenance. Firstly, the strong sub-harmonic at 640 GHz on the RF spectrum in Fig. 4(a) reveals misalignment of the MUX stages while the low 1.28 THz optical tone of the RF spectrum in Fig. 4(b) indicating signal distortion due to dispersion. These monitoring features were fed back to optimize the transmitter system to mitigate the impairments. The 640 GHz sub-harmonic tone was suppressed by optimizing the time delay and amplitude of the input data streams in the multiplexing stages and dispersion was compensated manually by adding dispersion compensating and standard single mode fibers. Figure 4(c) demonstrates the RF spectrum of an optimized 1.28 Tbit/s output signal, where the 640 GHz clock tone was eliminated and dispersion was minimized, indicated by the maximum power of the 1.28 THz tone. Note that the ripples on the RF spectrum are due to the broad width of the data signal pulses, which led to interference between adjacent pulses. To confirm the accuracy of the measured RF spectra we compared the autocorrelation generated from the inverse Fourier transform of the RF spectrum to that from a second-harmonic generation (SHG) autocorrelator for both the un-optimized and optimized 1.28 Tbit/s signal [Fig. 4(d) and 4(e)]. The reconstructed waveforms show good agreement with the traces from the SHG autocorrelator, highlighting the accuracy of the RF spectral measurement.

#126238 - $15.00 USD Received 30 Mar 2010; revised 11 Jul 2010; accepted 16 Jul 2010; published 29 Jul 2010

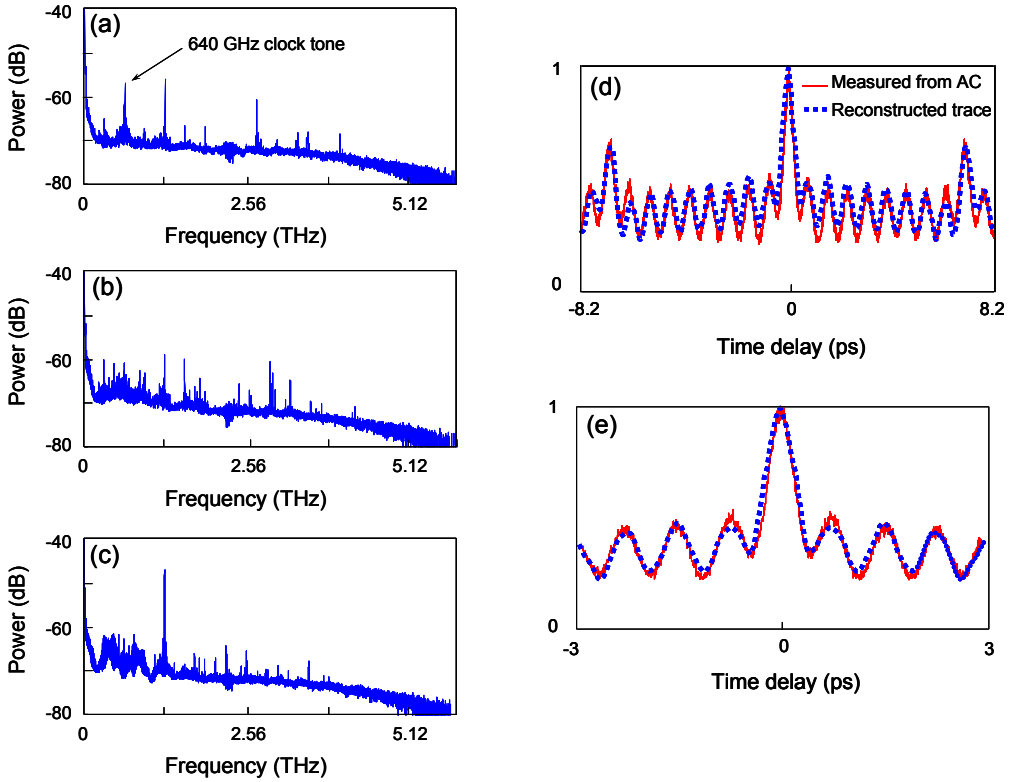

Fig. 4. The captured RF spectra showing (a) OTDM MUX misalignment, (b) distortion due to dispersion and (c) optimization of the Tbaud signal. The reconstructed AC waveforms of the (d) un-optimized and (e) optimized 1.28 Tbit/s signal (solid and dotted lines show the AC traces measured from the conventional autocorrelator and reconstructed from the captured RF spectra, respectively).

At the receiver, the high bit-rate OTDM signal was demultiplexed to the base rate via FWM inside the ChG chip. To characterize the FWM performance of this ChG waveguide, the control pulses were co-propagated with a tunable CW probe, whose wavelength was varied from 1530 nm to 1557 nm as shown in Fig. 5(a). Near uniform FWM conversion efficiency was obtained over 12 nm, whilst the 3 dB bandwidth of the gain envelop extended over 18 nm, highlighting the broadband phase-matching achieved by the dispersion-engineered waveguide.

The input AC waveform and eye diagram of the 1.28 Tbit/s signal is shown in Fig. 5(b) and 5(c) respectively (the AC graph also includes the AC of the 10 GHz control pulses for comparison). The full-width at half maximum of the 1.28 Tbit/s and the 10 GHz control pulses was ~370 fs and ~450 fs, respectively. Note, although the width of the pump pulses was slightly broader than the signal width, they only overlap with one data channel at a time.

#126238 - $15.00 USD Received 30 Mar 2010; revised 11 Jul 2010; accepted 16 Jul 2010; published 29 Jul 2010

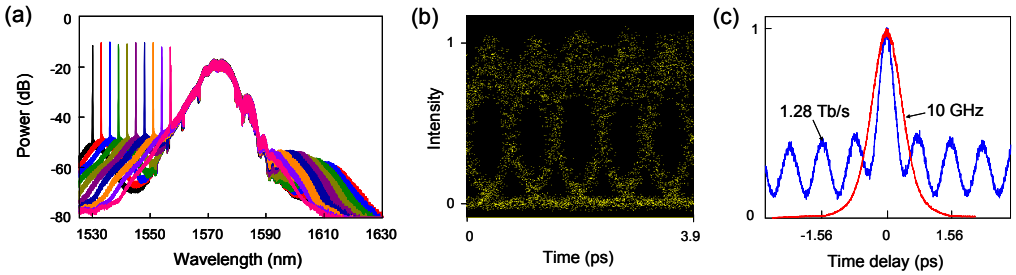

Fig. 5. (a) Optical spectra for various cw probe wavelengths, showing a broad FWM bandwidth. (b) Eye diagram and (c) AC trace of a 1.28 Tbit/s signal and AC trace of 10 GHz pulses.

Figure 6(a) shows the optical spectra of the 1.28 Tbit/s source signal and 10 GHz control pulses at the input and output of the waveguide. The FWM conversion efficiency of the 10 Gbit/s demultiplexed (demuxed) channel was calculated to be ~60% by integrating the powers of the optical spectra for the 1.28 Tbit/s input signal and output idler (taking the 128 times difference in bit-rate into account). Figure 6(b) shows the results of modeling the optical spectrum at the output of the waveguide using the split-step Fourier method [26] which predicts a FWM conversion efficiency of ~69% (with the same experimental parameters for waveguide, signal and control pulses without noise and polarization effects), in good agreement with the experimental result.

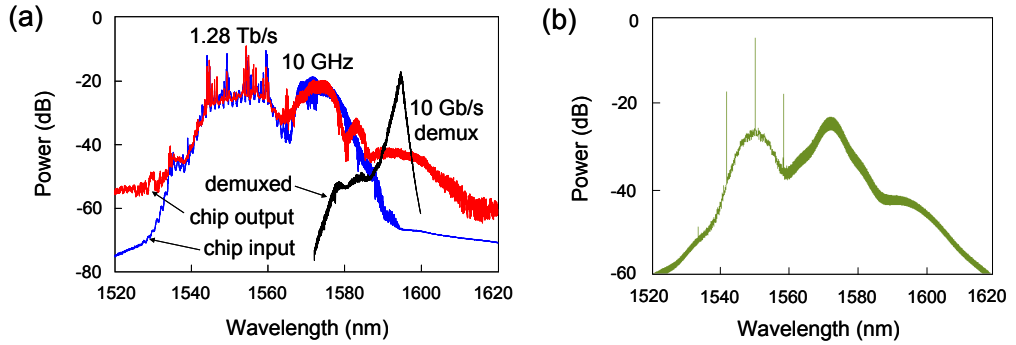

Fig. 6. (a) Experimental results showing the optical spectra at the input, output of the waveguide and before optical receiver. (b) Numerical result of the optical spectrum at the output of the waveguide.

The high quality of the idler signal generated by FWM is illustrated by the eye diagrams and BER measurements shown in Fig. 7(a). In this experiment, the 10 Gbit/s demultiplexed signal was located in the L-band. For a fair comparison, we therefore used a back-to-back (B2B) data signal at 10 Gbit/s, that had been converted to L-band. The eye diagram of the demultiplexed signal shows a clear opening with only marginally more noise than the B2B signal. The power penalty compared to the B2B signal was negligible at a BER of 10^{-9} (error-free level) as is illustrated in Fig. 7(a) for three adjacent channels of the 1.28 Tbit/s signal. These results demonstrate the excellent performance when demultiplexing a 1.28 Tbit/s data stream exhibiting negligible degradation of signal quality and without any indication of an error-floor in BER measurements. Note that ~5 dB power penalty between the demultiplexed channels and B2B C-band measurement was due to different performance of C- and L-band receivers. Finally, the received powers for 35 of the remaining channels at the error-free level were measured and are shown in Fig. 7(b), indicating a worst-case power penalty of ~5 dB.

#126238 - $15.00 USD Received 30 Mar 2010; revised 11 Jul 2010; accepted 16 Jul 2010; published 29 Jul 2010

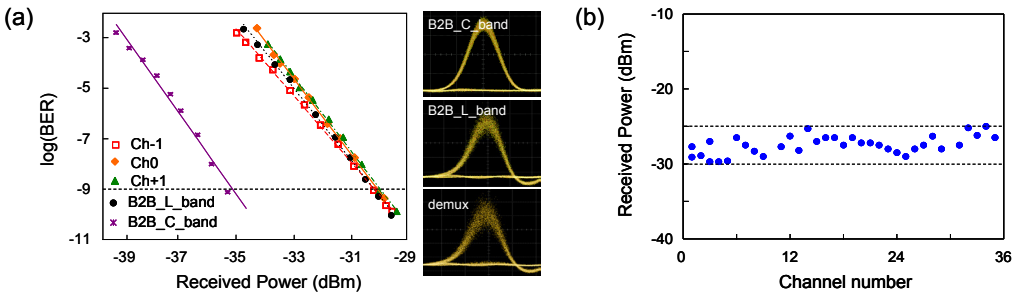

Fig. 7. (a) BER measurements and corresponding eye-diagrams of B2B and demultiplexed to 10 Gbit/s signals. (d) Receiver sensitivities at error-free level for demultiplexing of another 35 data channels

5. Discussion

Two crucial parameters for high bit-rate all-optical performance monitoring and demultiplexing are the pump-to-signal walk-off and the efficiency of the FWM process. Previous experiments have shown that the bandwidth of the ChG waveguide is greater than 2.5 THz [19]. It is therefore an ideal platform for OPM of Tbit/s signals. The FWM conversion efficiency is critical for the demultiplexing performance at the receiver and it is therefore important, to find the optimal value by balancing key parameters, including waveguide length, and pump power. We define the FWM conversion efficiency as the ratio between the generated idler and the input power of the signal. It can thus be written as [30]

$$\frac{P_{idler}(L)}{P_{signal}(0)} = \eta\gamma^2 P_0^2 e^{-\alpha L}\left(\frac{\left(1-e^{-\alpha L}\right)^2}{\alpha^2}\right) \tag{1}$$

where P_0 is the peak power of the pump, α is the propagation loss and η the FWM coefficient defined as [30]

$$\eta = \frac{\alpha^2}{\alpha^2+\Delta\beta^2}\left(1+\frac{4e^{-\alpha L}\sin^2(\Delta\beta.L/2)}{\left(1-e^{-\alpha L}\right)^2}\right) \tag{2}$$

with the phase-matching

$$\Delta\beta = \frac{2\pi\lambda^2}{c}\Delta f^2\left(D+\frac{\lambda^2}{c}.\Delta f.S\right) \tag{3}$$

here λ is the pump wavelength and Δf is the frequency difference between the signal and pump pulses.

Figure 8(a) shows the calculated FWM conversion efficiency as a function of waveguide length (using P_0 = 3 W and α = 0.5 dB/cm) which predicts a value of 77% for our 7-cm waveguide agreeing well with our numerical and experimental results. Although longer waveguides are available, including 14 and 21 cm, they offer lower conversion efficiency of only ~60% and ~25%, respectively due to both higher insertion loss and dispersion. Figure 8(b) shows the FWM conversion efficiency as a function of signal wavelength and peak power of the pump (with L = 7 cm and λ_{pump} = 1573 nm). This graph indicates the optimal signal wavelength with the corresponding pump power in order to achieve the highest FWM conversion efficiency. It can be seen that our experiment was well optimized for the available pump power of P_0 ~3 W. Note that a further increase in FWM conversion efficiency is possible by increasing the peak power. However, this not only exceeds the power handling of the chip but also spectrally broadens the pump pulses due to SPM, leading to spectral overlap between signal and pump.

#126238 - $15.00 USD Received 30 Mar 2010; revised 11 Jul 2010; accepted 16 Jul 2010; published 29 Jul 2010

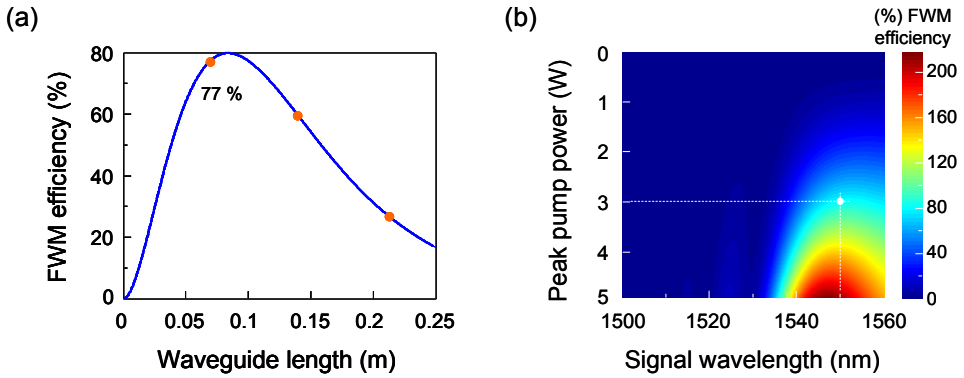

Fig. 8. (a) FWM conversion efficiency as a function of a waveguide length. (b) A function between a wavelength of an input signal and peak power of control pulses.

The current FWM conversion efficiency and performance of the device can be further improved by increasing the nonlinear coefficient γ and, most importantly, reducing loss of the waveguide. The waveguide nonlinearity can be improved with higher third order optical nonlinearity n_2 [31]. Free-space coupling loss, which is the main contribution to the total insertion loss of a waveguide, can be significantly reduced by exploiting the use of more efficient coupling techniques [32–34].

6. Conclusion

We have demonstrated, for the first time, a scheme for Tbit/s networks involving transmitter optimization and receiver-end demultiplexing via Tbaud all-optical signal processing on a compact photonic chip. The quality of the 1.28 Tbit/s OTDM signal at the transmitter was effectively monitored using a photonic chip based RF spectrum analyzer and used for impairment mitigation. At the receiver, the Tbit/s signal was successfully and all-optically demultiplexed using FWM and error-free performance was achieved with a very low power penalty (< 0.5 dB). Both Tbaud transmitter monitoring and receiver demultiplexing have been performed in a highly nonlinear, dispersion-shifted ChG planar waveguide. The proposed scheme could easily be extended to include multi-impairment monitoring and mitigation at intermediate nodes of a network.

Acknowledgements

This work was supported by an Australian Research Council (ARC) under the ARC Centres of Excellences and Linkage Programs.

#126238 - $15.00 USD Received 30 Mar 2010; revised 11 Jul 2010; accepted 16 Jul 2010; published 29 Jul 2010